Relationship of Titania Nanotube Binding Energies and Raman Spectra

Dana L. Morgan*, Eric R. Waclawik, and Ray L. Frost
Inorganic Materials Research Program, School of Physical and Chemical Sciences
Queensland University of Technology, GPO Box 2434, Brisbane, QLD 4001, Australia
* Author to whom correspondence should be addressed. Email: dl.morgan@qut.edu.au

Abstract— **Novel nanostructured titania nanotubes and hydrogen titanate nanoribbons were synthesised using hydrothermal treatment of Degussa P25. The nanostructure types formed were monitored as a function of the hydrothermal conditions. Changes in structure was evaluated using X-ray photoelectron spectroscopy (XPS), powder X-ray diffraction (XRD), Transmission electron microscopy (TEM) and Raman spectroscopy. X-ray photoelectron spectroscopy (XPS) of Ti($2p^{3/2}$) and O(1s) binding energies in titania nanotubes were measured and a systematic trend in the XPS binding energies was observed. This indicated a strengthening of the Ti-O bond occurred as the material phase changed from titania nanotube to the titanate ribbon form. The changes in binding energies for both the Ti and O XPS peaks were consistent with changes observed in the Raman spectra of nanostructured titania.**

Keywords-nanotube; nanoribbon; titania; titanate; soft-chemical hydrothermal treatment.

I. INTRODUCTION

Low-dimension forms of metal oxides have received considerable attention recently because controlled manipulation of a metal oxide's nanostructure can significantly change its chemical and electro-optical properties. Qualities inherent to metal oxides are also transferable to their nanostructured forms and this permits the incremental tailoring of these properties to specific applications [1]. Titanium dioxide (TiO_2), a wide-band gap semiconductor, is one of many metal oxides currently under investigation. It is readily converted into different nanostructured forms, including nanotubes. Potential applications of titania nanotubes include: gas sensors, ion-storage devices, environmental purification (including photocatalysis) and in biomedicine [2, 3].

Although there are multiple methods of titania nanotube production (replication, templating, anodic oxidation), nanotubes are most easily synthesised through a simple hydrothermal treatment [2, 4]. This so called "soft-chemical" treatment, developed by Kasuga *et al*. involves the conversion of a titania particle precursor in caustic solution at raised temperatures into nanotubes, reproducibly, and with consistent composition and dimensions [2-4]. The main advantage in converting particulate precursors into nanotubes is the ease and speed of synthesis from a common starting material. Titania nanotubes have been successfully formed from anatase and rutile starting material [5-7], however, nanotube formation from titanate precursors has been unsuccessful [8], unless aqueous hydrothermal treatment has been used [9].

Nanotube formation from soft-chemical treatment is considered to occur by delamination and subsequent 'rolling-up' of precursor nanosheets into scrolled nanotubes [10]. These rolled lamellar sheets are believed to undergo subsequent condensation and polymerisation, where the titania material's octahedral Ti-O building blocks are reassembled though reactions at hydroxy- and oxo-bridging sites (along (100) and (001) directions respectively) in the aqueous solution [1, 11]. Finally, open-ended nanotubes form through destabilisation of the sheet by saturation of 'dangling' bonds. Synthesis of 'onion-like' and concentric nanotube formations are also possible, depending upon reaction conditions [12, 13]. The 'onion-like' formation is believed to form through the curving of several conjoined nanosheets, producing a defect (seam) along one side of the nanotube. This is often observed experimentally. Nanotubes are not the only nanostructure formed through this hydrothermal treatment, titanate nanoribbons[1] also form under certain hydrothermal conditions [12, 14].

Phase and composition of the nanotubes is a key area of dispute within the current literature, where the nanostructure's phase is usually assigned to either a titania or a titanate species [10, 11, 15-17]. Chen *et al*. have used computer modelling as an aid in the determination of a simulated XRD profile using a trititanate nanotube model [16, 17]. This work has been the foundation of indexing the nanotube phase to a titanate species. Tsai *et al*. have argued that the nanotubes can be converted between titanate and anatase TiO_2 phases by the introduction and removal of NaOH, suggesting that the phases are interchangeable [15]. This mechanism is in agreement with recent work and statements of Kasuga *et al*. [3].

X-ray diffraction (XRD), Raman spectroscopy and electron diffraction studies are usually used to characterise titania nanotubes. The results obtained by both techniques are often affected by broadening and displacement of bands and reflections due to finite size effects. Therefore precise indexing of phase by XRD and Raman may be compromised. Also, Raman spectra obtained do not correlate directly to titania or titanate species and few studies have attempted to assign the new frequencies observed [18]. Other studies have

[1] Otherwise referred to as nanofibers, nanorods, and nanobelts.

used electron energy loss spectroscopy (EELS), X-ray photoelectron spectroscopy (XPS), Infrared spectroscopy (IR), solid state (Na, Li) and proton NMR to characterise nanostructured titania. Although these techniques have not been used extensively, interesting results have been obtained. EELS studies have assigned titania nanotube phase to anatase and rutile [10, 19], and have shown that the nanotubes contain no residual Na^+ [20]. IR studies have indicated that –OH and water is present in the samples [16, 18, 21, 22]. However, these results are not definitive for titanates, as TiO_2 species are known to have –OH defects on their surfaces and the nanotubes are also hydroscopic. Notably, few researchers have coupled thermogravimetric studies to their IR studies.

XPS has rarely been used in the examination of titania nanotubes [23, 24], though it has been used to examine other titania nanostructures, especially when metal-doped [1, 25, 26]. Although XPS is a surface analysis technique it is essentially a bulk technique in the examination of nanotubes due to the sampling depth being greater than the cross-section of the nanotube. Therefore, it has potential use in the determination of nanotube phase as well as compositional analysis. XPS allows for the examination of elemental constituents within a sample. In the case of TiO_2 both Ti^{4+} and O^{2-} species will be observed with typical binding energies. Shifts in binding energies can be caused by changes in the bond environment (i.e. strength of bond). For example: the Ti ($2p^{3/2}$) binding energies for $Na_2Ti_6O_{13}$ and TiO_2 are 458.1 and 458.9 eV respectively [27]. Although the shift is small, it does represent the strengthening and shortening of the Ti-O bond in the titanate crystal structure compared to TiO_2.

II. Experimental

A. Reagents and Synthesis

Titanium dioxide powder (Degussa P25), sodium hydroxide (Chem-Supply, 98 % purity), and hydrochloric acid (Univar, AR reagent, 32 w/w %) were all used without further purification. All solutions were prepared in ultra pure water (conductivity: 18.2 MΩ cm^{-1}).

Approximately 0.4g of titanium dioxide (Degussa P25) was treated with 30 – 35 mL NaOH solution through a soft-chemical hydrothermal treatment based on Kasuga *et al*. [4]. These solutions were sealed in PTFE-lined Parr bombs and statically heated in a SEM Convectional Oven for 20 hours. The resultant powder was washed with 0.1 M HCl and deionised H_2O through repetitive centrifugation until the supernatant was pH 7. The conditions chosen for this study were selected from a previous study, and were chosen to include nanoparticles, nanotubes, and nanoribbons [28]. For the specific hydrothermal conditions selected see Table 1.

B. Characterisation

Characterisation of the TiO_2 powders was achieved through powder X-ray diffraction (XRD), X-ray photoelectron spectroscopy (XPS) and Raman spectroscopy. Morphological characterisation was achieved through transmission electron microscopy (TEM). All XRD patterns were obtained using a Philips PANalytical X'Pert PRO X-ray diffractometer operating at 40 kV and 40 mA using Cu-Kα_1 radiation λ = 1.54 Å. Analysis of sample through Bragg-Brentano geometry was utilised from 20 – 70° 2θ. XPS was achieved with a Kratos Axis ULTRA X-Ray Photoelectron Spectrometer incorporating a 165 nm hemispherical electron energy analyser. Monochromatic Al X-rays (1486.6 eV) at 150 W (15 kV, 10 mA) was utilised as the incident radiation. Multiplex high resolution scans where achieved at an analyser pass energy of 20 eV in 0.10 eV steps. Raman spectroscopy was performed on a Renishaw In-Via Raman microscope coupled to a Leica microscope using a Renishaw double Nd:YAG laser to produce 532 nm excitation radiation. The samples were analysed from 50 – 1200 cm^{-1} with Rayleigh rejection achieved through a 532 nm Laser RSSF notch filter. TEM examination and analysis was carried out on a Philips CM200 TEM operated at 200 kV.

III. Results and Discussion

As the aim of this study was to establish whether XPS could be used as a phase determining tool, XPS measurements were performed in tandem with XRD and Raman studies. Although the differences in binding energies between titanate and titania phases were small, XPS resolution and sensitivity was high enough to measure the binding energy changes. To determine possible correlations between Raman and XPS the samples were listed in order of increase of Ti ($2p^{3/2}$) binding energy and the spectra were plotted in this order (See Table 1).

TABLE I. Nanostructure Binding Energies And Morphology

Sample	Hydrothermal Conditions	Binding Energy (eV)[a]		Morphology
		Ti ($2p^{3/2}$)	*O (1s)*	
A	9 M @ 200°C	458.2	529.8	Nanoribbon
B	10 M @ 140°C	458.5	530.0	Nanotube
C	5 M @ 220°C	458.6	530.1	Nanotube/ Nanoribbon
D	9 M @ 160°C	458.9	530.4	Nanotube
E	7.5 M @ 100°C	458.9	530.4	Nanotube/ Nanoparticle

a. Charge Correction: Adventitious Carbon (284.8 eV)

Various titania-based nanostructures were examined, including: nanotubes, nanoribbons and nanoparticles (Figure 1). A typical nanotube specimen consisted of 10 nm ± 2 nm diameter tubes and a range of lengths (100 nm – 400 nm). A TEM image of a hydrothermally produced titania nanotube sample is presented in Figure 1a. The nanotubes are amorphous, producing a diffuse ring small area electron diffraction (SAED) pattern (Figure 1 inset). The difference in size dimensions of the nanotubes and nanoribbons is evident in Figure 1b where both morphologies were observed. The nanoribbon's average widths were approximately 150 nm and >1.6 μm in length. In comparison to the nanotubes whose walls created contrast in the TEM images, the nanoribbons appeared flat and no internal structure could be discerned in initial TEM image analysis. Upon closer examination however, the nanoribbons in Figure 1c were found to possess an internal structure consisting of flat, multilayered plates.

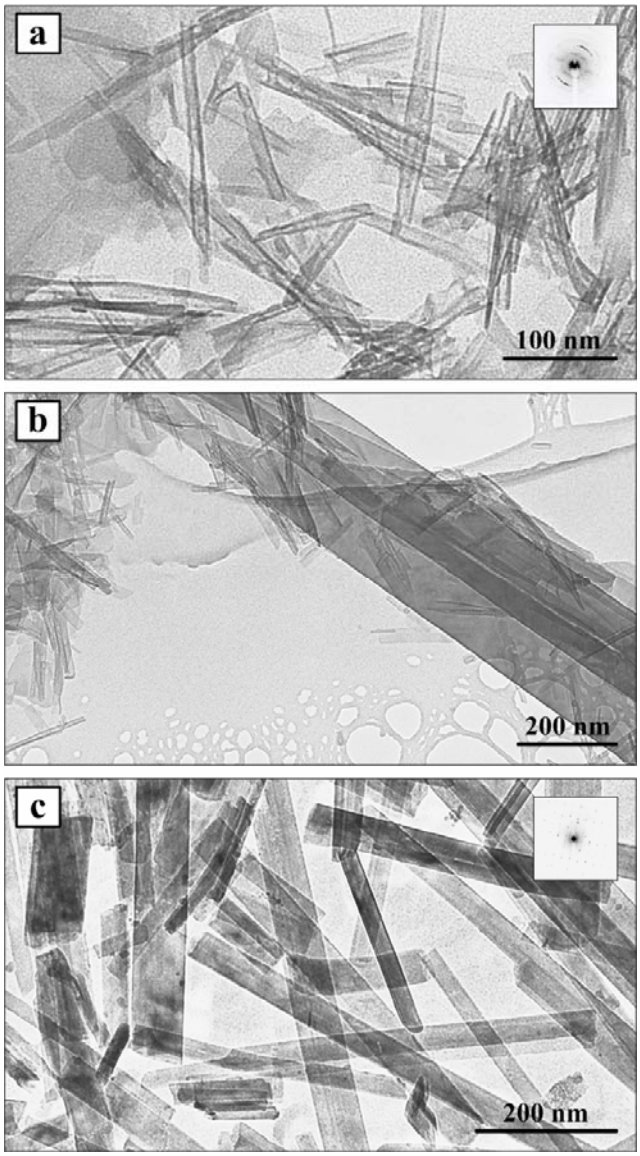

Figure 1. TEM Images: (a) Nanotubes synthesised at 5 M @ 220°C, SAED inset; (b) Nanotubes and nanoribbons synthesised at 5 M @ 220°C; (c) Nanoribbons synthesised at 9 M @ 200°C, SAED inset.

These plate-like structures are consistent with a monoclinic structure or phase, which was confirmed with the quantitative assignment of the SAED pattern of this image to $H_2Ti_5O_{11}$•$3H_2O$ (PDF # 44-0130). From this figure it was evident that nanoribbons vary in size significantly with wide distributions in both width (10 – 120nm) and length (90 – 850 nm) for an individual batch.

Changes in the phase and morphology of the nanostructures are clearly evident in the Raman spectra (Figure 2). Sample A, the nanoribbon sample, has a Raman spectrum similar to a titanate-species, albeit with partially resolved peaks in comparison to known sodium titanates [29]. Samples B – D produced Raman spectra typically observed for titania nanotubes. Sample E contains anatase and a secondary phase. When the Raman spectra are ordered via the binding energy several spectral features are observed to evolve. The most obvious of these features is the doublet that appears

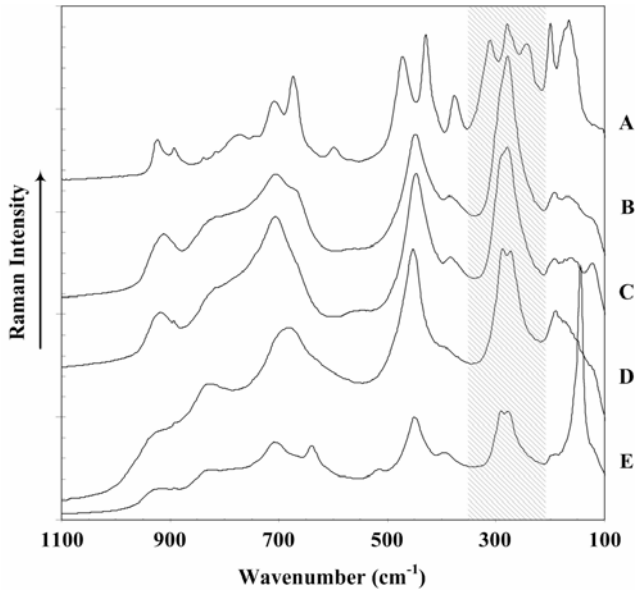

Figure 2. Raman Spectra of Samples

between 320 – 220 cm^{-1} initially observed in Sample E. This doublet increases in intensity from Sample E to D through an unresolved doublet in Sample C which loses further resolution in Sample B. This singlet then splits into a resolved triplet in Sample A. This transition in this spectral region appears to correlate closely to the increase in binding energy.

Anatase, is the predominate phase within Sample E, as evident from the strong intensities of the anatase E_g and A_g bands at 140 and 510 cm^{-1} respectively. The presence of these frequencies indicates that a large amount of unreacted starting material was still present in the sample. The doublet and other non-anatase peaks in the spectra indicate the presence of nanotube scrolls (confirmed through TEM studies). The absence of typical anatase frequencies in Sample D indicates that no starting material remained following harsher hydrothermal reaction conditions. The form that this sample's Raman spectrum takes would therefore be likely to arise from titania nanotubes only, resulting in a typical nanotube spectrum. Between Samples B – D there are minor variations in frequencies and intensities which are commonly observed for most nanotube samples. Samples B and C display some vibrations similar to those observed in Sample A. These include the increase in resolution of a shouldering peak arising at *ca*. 380 cm^{-1} and the shift and formation of peaks between 960 – 610cm^{-1} from Sample D through B. The presence and increase in intensity of peaks at these wavelengths may indicate that that the samples phases and therefore Raman spectra are gradually becoming more titanate-influenced. The peak at 906 cm^{-1} observed in Samples C and D was assigned by Qian *et al*. as a symmetric stretching mode of short Ti-O bonds which is characteristic of parent sodium compounds [18]. When comparing these spectra with the binding energies it is interesting to note that those observed for Samples C through E are within the observed energies for TiO_2. The presence of the peak-shoulders observed in Samples B and C and an observed increase in binding energy suggests that the phase is taking on titanate character. However we note that the binding energy values for Samples B and C remain more intermediate TiO_2-

like than binding energies characteristic of a true titanate phase [27]. The analysis of Raman spectrum changes indicate that the reduced peak resolution of the doublet frequencies in the 320 – 220 cm^{-1} range from Sample E to A are related to Ti-O vibrations. The progression in peak shape and increase in binding energy indicates a strengthening in the associated bond. Qian *et al*. relate the peak in this region to a Ti-OH bond which is integral to the formation and stability of the tubular structure of the TiO_2 nanotube [18].

IV. Conclusions

Raman results indicate that there is a definite phase change observed between the samples analysed, which can be attributed to alterations in the morphology and subsequent phase of the samples. The transition of strength and resolution of a doublet formation within the 320 – 220 cm^{-1} range, appears to correlate to the increase in binding energy of both Ti ($2p^{3/2}$) and O (1s) bands. This suggests that these frequencies do relate to Ti-O bonds which strengthen when the nanostructure alters from nanoparticles through nanotubes to nanoribbons. The binding energies also indicate that the nanotubes are more TiO_2-like than titanate-like in nature.

Acknowledgment

The authors would like to thank Dr Barry Wood from the Brisbane Surface Analysis Facility at the University of Queensland for the use of their XPS which QUT has access through a LEIF agreement.

References

[1] A. Chemseddine and T. Moritz, "Nanostructuring titania: control over nanocrystal structure, size, shape and organisation," *European Journal of Inorganic Chemistry*, pp. 235-245, 1999.

[2] T. Kasuga, M. Hiramatsu, A. Hoson, T. Sekino, and K. Niihara, "Formation of titanium oxide nanotube," *Langmuir*, vol. 14, pp. 3160-3163, 1998.

[3] T. Kasuga, "Formation of titanium oxide nanotubes using chemical treatments and their characteristic properties," *Thin Solid Films*, vol. 496, pp. 141-145, 2006.

[4] T. Kasuga, M. Hiramatsu, A. Hoson, T. Sekino, and K. Niihara, "Titania nanotubes prepared by chemical processing," *Advanced Materials*, vol. 11, pp. 1307-1311, 1999.

[5] Y. Lan, X. Gao, H. Zhu, Z. Zheng, T. Yan, F. Wu, S. P. Ringer, and D. Song, "Titanate nanotubes and nanorods prepared from rutile powder," *Advanced Functional Materials*, vol. 15, pp. 1310-1318, 2005.

[6] A. Thorne, A. Kruth, D. Tunstall, J. T. S. Irvine, and W. Zhou, "Formation, structure, and stability of titanate nanotubes and their proton conductivity," *Journal of Physical Chemistry B*, vol. 109, pp. 5439-5444, 2005.

[7] Y. Zhu, H. Li, Y. Koltypin, Y. R. Hacohen, and A. Gedanken, "Sonochemical synthesis of titania whiskers and nanotubes," *Chemical Communications*, vol. 24, pp. 2616-2617, 2001.

[8] A. Kukovecz, M. Hodos, E. Horvath, G. Radnoczi, Z. Konya, and I. Kiricsi, "Oriented crystal growth model explains the formation of titania nanotubes," *Journal of Physical Chemistry B*, vol. 109, pp. 17781-17783, 2005.

[9] M. Wei, Y. Konishi, H. Zhou, H. Sugihara, and H. Arakawa, "Formation of nanotubes TiO_2 from layered titanate particles by a soft chemical process," *Solid State Communications*, vol. 133, pp. 493-497, 2005.

[10] Y. Q. Wang, G. Q. Hu, X. F. Duan, H. L. Sun, and Q. K. Xue, "Microstructure and formation mechanism of titanium dioxide nanotubes," *Chemical Physics Letters*, vol. 365, pp. 427-431, 2002.

[11] W. Wang, O. K. Varghese, M. Paulose, and C. A. Grimes, "A study on the growth and structure of titania nanotubes," *Journal of Materials Research*, vol. 19, pp. 417-422, 2004.

[12] D. V. Bavykin, V. N. Parmon, A. A. Lapkin, and F. C. Walsh, "The effect of hydrothermal conditions on the mesoporous structure of TiO_2 nanotubes," *Journal of Materials Chemistry*, vol. 14, pp. 3370-3377, 2004.

[13] J. Yang, Z. Jin, X. Wang, W. Li, J. Zhang, S. Zhang, X. Guo, and Z. Zhang, "Study on composition, structure and formation process of nanotube $Na_2Ti_2O_4(OH)_2$," *Dalton Transactions*, pp. 3898-3901, 2003.

[14] D. Wu, J. Liu, X. Zhao, A. Li, Y. Chen, and N. Ming, "Sequence of events for the formation of titanate nanotubes, nanofibers, nanowires and nanobelts," *Chemistry of Materials*, vol. 18, pp. 547-553, 2006.

[15] C.-C. Tsai and H. Teng, "Structural features of nanotubes synthesised from NaOH treatment of TiO_2 with different post-treatments," *Chemisty of Materials*, vol. 2006, pp. 367-373, 2006.

[16] Q. Chen, G. H. Du, S. Zhang, and L.-M. Peng, "The structure of trititanate nanotubes," *Acta Crystallographica*, vol. B58, pp. 587 - 593, 2002.

[17] Q. Chen, W. Z. Zhou, G. H. Du, and L.-M. Peng, "Trititanate nanotubes made via a single alkali treatment," *Advanced Materials*, vol. 14, pp. 1208-1211, 2002.

[18] L. Qian, Z.-L. Du, S.-Y. Yang, and Z.-S. Jin, "Raman study of titania nanotube by soft chemical process," *Journal of Molecular Structure*, vol. 749, pp. 103-107, 2005.

[19] T. Akita, M. Okumura, K. Tanaka, K. Ohkuma, M. Kohyama, T. Koyanagi, M. Date, S. Tsubota, and M. Haruta, "Transmission electron microscopy observation of the structure of TiO_2 nanotube and Au/TiO_2 nanotube catalyst," *Surface and Interface Analysis*, vol. 37, pp. 265-269, 2005.

[20] R. Ma, Y. Bando, and T. Sasaki, "Directly Rolling Nanosheets into Nanotubes," *Journal of Physical Chemistry B*, vol. 108, pp. 2115-2119, 2004.

[21] X. Sun and Y. Li, "Synthesis and characterization of ion-exchangeable titanate nanotubes," *Chemistry--A European Journal*, vol. 9, pp. 2229-2238, 2003.

[22] X.-P. Tang, K. C. Chartkunchand, and Y. Wu, "A novel nuclear spin-lattice relaxation filter for separating the free and absorbed water in a matrix of titanate nanotubes," *Chemical Physics Letters*, vol. 399, pp. 456-460, 2004.

[23] C. Ruan, M. Paulose, O. K. Varghese, G. K. Mor, and C. A. Grimes, "Fabrication of highly ordered TiO_2 nanotube arrays using an organic electrolyte," *Journal of Physical Chemistry B*, vol. 109, pp. 15754-15759, 2005.

[24] J.-C. Xu, M. Lu, X.-Y. Guo, and H.-L. Li, "Zinc ions surface-doped titanium dioxide nanotubes and its photocatalysis activity for degradation of methyl orange in water," *Journal of Molecular Catalysis A: Chemical*, vol. 226, pp. 123-127, 2005.

[25] M. Andersson, L. Österlund, S. Ljungström, and A. Palmqvist, "Preparation of nanosize anatase and rutile TiO_2 by hydrothermal treatment of microemulsions and their activity for photocatalytic wet oxidation of phenol," *Journal of Physical Chemistry B*, vol. 106, pp. 10674-10679, 2002.

[26] S. Hwang, M. C. Lee, and W. Choi, "Highly enhanced photocatalytic oxidation of CO on titania deposited with Pt nanoparticles: kinetics and mechanism," *Applied Catalysis B: Environmental*, vol. 46, pp. 49-63, 2003.

[27] "NIST X-ray Photoelectron Spectroscopy Database." http://srdata.nist.gov/xps, Last accessed 18/06/2006.

[28] D. L. Morgan, "Synthesis, characterisation and photocatalytic studies of titania nanotubes," in *School of Physical and Chemical Sciences*. Brisbane: Queensland University of Technology, 2004, pp. 81.

[29] C. E. Bamberger and G. M. Begun, "Sodium titanates: stoichiometry and Raman spectra," *Journal of the American Ceramic Society*, vol. 70, pp. C48-C51, 1987.